

Self-assembled Pt₂L₂ boxes strongly bind G-quadruplex DNA and influence gene expression in cancer cells.

O. Domarco,^a D. Lötsch,^b J. Schreiber,^b C. Dinhof,^b S. Van Schoonhoven,^b M. D. García,^a C. Peinador,^{*a} B. K. Keppler,^{c,d} W. Berger,^{b,d} and A. Terenzi^{*c,d}

^a*Universidad da Coruña, Departamento de Química Fundamental and Centro de Investigacións Científicas Avanzadas, Facultade de Ciencias, E-15071 A Coruña, Spain*

^b*Medical University Vienna, Department of Medicine I, Institute of Cancer Research and Comprehensive Cancer Center, Borschkegasse 8a, A-1090 Vienna, Austria.*

^c*University of Vienna, Institute of Inorganic Chemistry, Waehringerstrasse 42, A-1090 Vienna, Austria.*

^d*Research Platform "Translational Cancer Therapy Research", University of Vienna and Medical University of Vienna, Vienna, Austria.*

Supporting Information

Methods and References	Pag. 2-8
Supplementary Figures	Pag. 9-17

Experimental

General

All chemicals, including 5,10,15,20-Tetrakis(1-methyl-4-pyridinio)porphyrin tetra(p-toluenesulfonate) (TMPyP), were purchased from Sigma Aldrich or Acros and used as received. Solvents were purchased as analytical grade and used without further purification. MilliQ water was used to prepare buffers and pH was measured using a Mettler Toledo pH meter.

Analysis and plotting of the data were carried out using Origin 9.5 (OriginLab Corp.) and GraphPad Prism (version 5; GraphPad Software, San Diego, CA).

Oligonucleotides and DNA

All oligonucleotides (standard and labelled with FRET couple) (see Table 1) were purchased from IDT (Integrated DNA Technologies) in HPLC purity grade. The FRET probes used were FAM (6-carboxyfluorescein) and TAMRA (6-carboxy-tetramethylrhodamine). As model for ds-DNA the TATAGCTA-Heg-TATAGCTATA sequence was used (Heg linker = $[(-\text{CH}_2-\text{CH}_2-\text{O})_6]$).

The concentration of the oligonucleotide stock solutions was checked measuring the absorbance at 260 nm of the corresponding diluted solutions using the extinction coefficient values provided by the manufacturer.

Lyophilized calf thymus DNA (ct-DNA, Sigma-Aldrich) was used as model for *ds-DNA* during UV-Vis and CD experiments. It was resuspended in 1.0 mM tris-hydroxymethyl-aminomethane (Tris-HCl) pH=7.5. DNA concentration was determined by UV spectrophotometry using $6600 \text{ M}^{-1} \text{ cm}^{-1}$ as molar absorption coefficient at 260 nm.¹

Table S1. 5'-3' sequences of the oligonucleotides used. In bold the 4 runs of guanines responsible of the quadruplex formation are shown.

Oligos	Sequence
<i>h-Telo</i>	AGG GTT AGG GTT AGG GTT AGG G
<i>c-Myc</i>	TGG GGA GGG TGG GGA GGG TGG GGA AGG
<i>c-Kit1</i>	AGG GAG GGC GCT GGG AGG AGG G
<i>h-TERT</i>	GGG GGC TGG GCC GGG GAC CCG GGA GGG GTC GGG ACG GGG CGG GG
<i>bcl2</i>	AGG GGC GGG CGC GGG AGG AAG GGG GCG GGA GCG GGG CTG
<i>TERRA</i>	UUA GGG UUA GGG UUA GGG UUA GGG
ds-DNA	TATAGCTATA-Heg-TATAGCTATA

Synthesis

Ligands **1**,² **3**³ and **5**⁴ and Pt boxes **2**,² **4**³ and **6**⁴ were prepared according to published procedures.

FRET studies

FRET experiment were performed in 96-well plates and run on an Applied Biosystems® 7500 Real-Time PCR cycler equipped with a FAM filter ($\lambda_{ex} = 492$ nm; $\lambda_{em} = 516$ nm).

The lyophilized strands were firstly diluted in MilliQ water to obtain 100 μ M stock solutions. These were diluted to a concentration of 400 nM in 60 mM potassium cacodylate buffer (pH 7.4) and then annealed to form G4 structures by heating to 95 °C for 5 min, followed by slowly cooling to room temperature overnight.

Experiments were carried out in a 96 well plate with a total volume of 30 μ l. Final concentration of the oligonucleotides was 200 nM. All compounds, including control TMPyP4, were previously dissolved in DMSO to give 1 mM stock solutions. These were further diluted using 60 mM potassium cacodylate, and added to obtain a final concentration of 1 μ M (with a total percentage of DMSO around 0.1 %).

Ramp temperature program was set with a stepwise increase of 1 °C every 30 s starting from 25 °C to reach 95 °C, and measurements were acquired after each step. To compare different sets of data, FAM emission data were normalised (0 to 1).⁵ $T_{1/2}$ is defined as the temperature at which the normalised emission is 0.5. Measurements were made in duplicate or triplicate.

UV-visible absorption

UV-vis spectra were collected on Jasco V-650 and PerkinElmer LAMBDA 35 double beam spectrophotometers, equipped the later with a Peltier temperature controller, and using 1 cm path-length quartz cuvettes. All experiments were carried in 100 mM KCl, 50 mM Tris-HCl aqueous buffer at pH=7.5.

The oligonucleotides were dissolved in MilliQ water to yield a 100 μ M stock solution. This was then diluted using 50 mM Tris-HCl/100 mM KCl buffer (pH 7.4) to the desired concentration. The oligonucleotides were folded by first heating the solutions up to 90 $^{\circ}$ C for 5 min and then by slowly cooling down to room temperature. Ct-DNA stock solution was diluted using 50 mM Tris-HCl/100 mM KCl buffer and used as it was.

UV-visible absorption spectra were recorded at 25 $^{\circ}$ C. The titrations were carried out by adding increasing amounts of DNA (ct-DNA or G4) solution to a Pt-box solution with constant concentration. To ensure that during the titration the concentration of the selected Pt-box remained unaltered, for each addition of the DNA solution the same volume of a double-concentrated Pt-box solution was added.

K_b values were obtained by fitting the UV data to a reciprocal plot of $[DNA]/|\epsilon_a - \epsilon_f|$ vs. $[DNA]$ using the equation $[DNA]/|\epsilon_a - \epsilon_f| = [DNA]/|\epsilon_b - \epsilon_f| + 1/(|\epsilon_b - \epsilon_f| \times K_b)$,⁶ where $\epsilon_a = A_{\text{observed}}/[Pt\text{-box}]$, ϵ_b is the extinction coefficient of the DNA bound Pt-box, and ϵ_f is the extinction coefficient of the free Pt-box determined by a calibration curve of the isolated Pt-box in aqueous solution, following the Beer–Lambert law.

Circular Dichroism

Circular dichroism spectra were recorded on Chirascan™ CD (by AppliedPhotophysics) or Jasco J-185 spectrometers, using 1 cm path-length quartz cuvettes, at 25 $^{\circ}$ C with the following parameters: range 500-200 nm, bandwidth: 1.0 nm, time per point: 0.5 s, repeats: 4. The titrations were carried out by adding increasing amounts of a Pt-box stock solution to a DNA/G4 solution with constant concentration. To ensure that during the titration the concentration of the DNA/G4 remained unaltered, for each addition of the Pt-box solution, the same volume of a double-concentrated DNA/G4 solution was added. To have an estimation of the K_b values, the ICD data were fitted using a “one site” non-linear regression model within the software GraphPad Prism (this was possible only in the case of the interaction between compounds **4** and **6** with ds-DNA, where clear ICD bands were observed).

Molecular Modelling

Molecular docking was performed by the software AutoDock Vina 1.1.2.⁷ The Protein Data Bank file PDB ID: 2O3M was used as model of *c-Kit1* -quadruplex receptor. To compare our results with the ones obtained by Kieltyka *et al.* for the compound [Pt(en)(4,4'-dipyridyl)]₄,⁸ PDB ID: 1KF1 was used as model of *hTelo*-quadruplex receptor.

The geometries of compounds **2**, **4** and **6**, to be used in the docking studies, were previously fully optimized by DFT calculations implemented in the Gaussian09 program package,⁹ using the B3LYP functional,¹⁰⁻¹² the Lanl2dz pseudopotential basis set for platinum,¹³ and the 6-31G(d,p) basis set for the other atoms.^{14,15}

The Autodock Tools 1.5.6 software was used to add and merge non-polar hydrogens to the receptors and to assign the rotatable bonds to the ligands.¹⁶ A grid box large enough to allow any possible ligand-receptor complex (blind-docking) was created. In particular, grid size for 2O3M was set to 30Å × 30Å × 26Å points with grid spacing of 1.0 Å and a grid center of -1.033, 2.235 and -1.266. Grid size for 1KF1 was set to 30Å × 30Å × 30Å points with grid spacing of 1.0 Å and a grid center of 23.505, -2.168 and -9.076. Before docking calculations, Pt(II) was changed with Ni(II) in the three compounds to retain the square planar coordination. Validation of AutoDock Vina was performed running a docking calculation on a parallel stranded human telomeric quadruplex in complex with the compound TMPyP4 (PDB ID: 2HRI),¹⁷ confirming the best pose of the ligand. Figures were rendered using Chimera software.¹⁸

Cell cultures

The MCF-7 breast cancer cells, as well as the U2OS osteosarcoma cell line were obtained from the American Type Culture Collection (Manassas, VA). VM-1 melanoma cells were established from a lymph node metastasis at the Institute of Cancer Research (Vienna, Austria).

Cell viability assay

Cancer cells were exposed to the Pt-boxes and to the corresponding 4,4'-bipyridine ligands at increasing concentrations and 72 hours later cell viability was determined using 3-(4,5-dimethylthiazol-2-yl)-2,5-diphenyltetrazolium bromide (MTT)-based vitality assay (EZ4U, Biomedica, Vienna, Austria). Response-rates were expressed as IC₅₀ values calculated with GraphPad Prism.

Cell cycle analysis

Cells were incubated with the Pt-boxes or with the ligands for 48 hours using 10 and 25 µM of each drug. Afterwards cells were trypsinized and fixed with 70% ethanol at -20°C for several hours, following DNA staining using a solution of PI (0.01 mg/ml) and RNase (0.2 mg/ml). Finally, cell cycle progression was examined by flow cytometry and quantified with FlowJo software (Tree Star).

Annexin V/PI staining

Apoptosis and necrosis were determined by Annexin V FITC-labelled antibody (BD Biosciences, San Jose, CA) and propidium iodide (Sigma Aldrich, USA), respectively. For that purpose, cells were treated with 25µM of the indicated drugs for 24 hours, subsequently trypsinized and incubated with the antibody and propidium iodide (200 ng/ml). Finally, DNA content and the amount of dead cells were measured by fluorescence-activated cell sorting (FACSCalibur, Becton Dickinson, Palo Alto, CA) and quantified with FlowJo software (Tree Star).

Quantitative reverse transcription-polymerase chain reaction (qRT-PCR)

Total RNA was extracted from cells using Trizol reagent (Life Technologies, Carlsbad, CA) and subsequently 500ng RNA per sample were reverse transcribed. qRT-PCR was performed with Maxima SYBR Green qPCR master mix (Thermo Scientific) on an Applied Biosystems 7500 Fast Real-Time PCR instrument (Applied Biosystems, Foster City, CA), as described earlier.^{19,20} The following primers were used: c-Kit1 (sense 5'-TCTCTGCGTTCTGCTCCTAC-3'; antisense 5'-GGTTGAGAAGAGCCTGTCTG-3'), bcl2 (sense 5'-CTTCGCCGAGATGTCCAGCCA-3'; antisense 5'-CGCTCTCCACACACATGACCC3'), hTERT (sense 5'-CGGAGGAGTGTCTGGAGCAA-3'; antisense 5'-GGATGAAGCGGAGTCTGGA-3') and β-actin (sense 5'-GGATGCAGAAGGAGATCACTG-3'; antisense 5'-CGATCCACACGGAGTACTTG -3'). β-actin served as housekeeping gene and was

used for normalization. All reactions were performed in triplicates and repeated independently at least twice.

References

- 1 M. E. Reichmann, S. A. Rice, C. A. Thomas and P. Doty, *J. Am. Chem. Soc.*, 1954, **76**, 3047–3053.
- 2 V. Blanco, M. Chas, D. Abella, E. Pia, C. Platas-Iglesias, C. Peinador and J. M. Quintela, *Org. Lett.*, 2008, **10**, 409–412.
- 3 V. Blanco, A. Gutierrez, C. Platas-Iglesias, C. Peinador and J. M. Quintela, *J. Org. Chem.*, 2009, **74**, 6577–6583.
- 4 E. M. Lopez-Vidal, V. Blanco, M. D. Garcia, C. Peinador and J. M. Quintela, *Org. Lett.*, 2012, **14**, 580–583.
- 5 D. Renčiuk, J. Zhou, L. Beaurepaire, A. Guédin, A. Bourdoncle and J.-L. Mergny, *Methods*, 2012, **57**, 122–128.
- 6 A. Wolfe, G. H. Shimer and T. Meehan, *Biochemistry*, 1987, **26**, 6392–6396.
- 7 O. Trott and A. J. Olson, *J. Comput. Chem.*, 2010, **31**, 455–61.
- 8 R. Kieltyka, P. Englebienne, J. Fakhoury, C. Autexier, N. Moitessier and H. F. Sleiman, *J. Am. Chem. Soc.*, 2008, **130**, 10040–10041.
- 9 M. J. Frisch, G. W. Trucks, H. B. Schlegel, G. E. Scuseria, M. A. Robb, J. R. Cheeseman, G. Scalmani, V. Barone, B. Mennucci, G. A. Petersson, H. Nakatsuji, M. Caricato, X. Li, H. P. Hratchian, A. F. Izmaylov, J. Bloino, G. Zheng, J. L. Sonnenberg, M. Hada, M. Ehara, K. Toyota, R. Fukuda, J. Hasegawa, M. Ishida, T. Nakajima, Y. Honda, O. Kitao, H. Nakai, T. Vreven, J. A. Montgomery Jr., J. E. Peralta, F. Ogliaro, M. Bearpark, J. J. Heyd, E. Brothers, K. N. Kudin, V. N. Staroverov, R. Kobayashi, J. Normand, K. Raghavachari, A. Rendell, J. C. Burant, S. S. Iyengar, J. Tomasi, M. Cossi, N. Rega, J. M. Millam, M. Klene, J. E. Knox, J. B. Cross, V. Bakken, C. Adamo, J. Jaramillo, R. Gomperts, R. E. Stratmann, O. Yazyev, A. J. Austin, R. Cammi, C. Pomelli, J. W. Ochterski, R. L. Martin, K. Morokuma, V. G. Zakrzewski, G. A. Voth, P. Salvador, J. J. Dannenberg, S. Dapprich,

- A. D. Daniels, Ö. Farkas, J. B. Foresman, J. V Ortiz, J. Cioslowski and D. J. Fox, *Gaussian Inc Wallingford CT*, 2009, 34, Wallingford CT.
- 10 A. D. Becke, *J. Chem. Phys.*, 1993, **98**, 5648–5652.
 - 11 C. Lee, W. Yang and R. G. Parr, *Phys. Rev. B*, 1988, **37**, 785–789.
 - 12 P. J. Stephens, F. J. Devlin, C. F. Chabalowski and M. J. Frisch, *J. Phys. Chem.*, 1994, **98**, 11623–11627.
 - 13 P. J. Hay and W. R. Wadt, *J. Chem. Phys.*, 1985, **82**, 270–283.
 - 14 P. C. Hariharan and J. A. Pople, *Theor. Chim. Acta*, 1973, **28**, 213–222.
 - 15 M. M. Francl, *J. Chem. Phys.*, 1982, **77**, 3654–3665.
 - 16 G. M. Morris, R. Huey, W. Lindstrom, M. F. Sanner, R. K. Belew, D. S. Goodsell and A. J. Olson, *J. Comput. Chem.*, 2009, **30**, 2785–2791.
 - 17 G. N. Parkinson, R. Ghosh and S. Neidle, *Biochemistry*, 2007, **46**, 2390–2397.
 - 18 E. F. Pettersen, T. D. Goddard, C. C. Huang, G. S. Couch, D. M. Greenblatt, E. C. Meng and T. E. Ferrin, *J. Comput. Chem.*, 2004, **25**, 1605–1612.
 - 19 B. Englinger, D. Lötsch, C. Pirker, T. Mohr, S. van Schoonhoven, B. Boidol, C.-H. Lardeau, M. Spitzwieser, P. Szabó, P. Heffeter, I. Lang, M. Cichna-Markl, B. Grasl-Kraupp, B. Marian, M. Grusch, S. Kubicek, G. Szakács and W. Berger, *Oncotarget*, 2016, doi: 10.18632/oncotarget.10324.
 - 20 H. Fischer, N. Taylor, S. Allerstorfer, M. Grusch, G. Sonvilla, K. Holzmann, U. Setinek, L. Elbling, H. Cantonati, B. Grasl-Kraupp, C. Gauglhofer, B. Marian, M. Micksche and W. Berger, *Mol. Cancer Ther.*, 2008, **7**, 3408–3419.

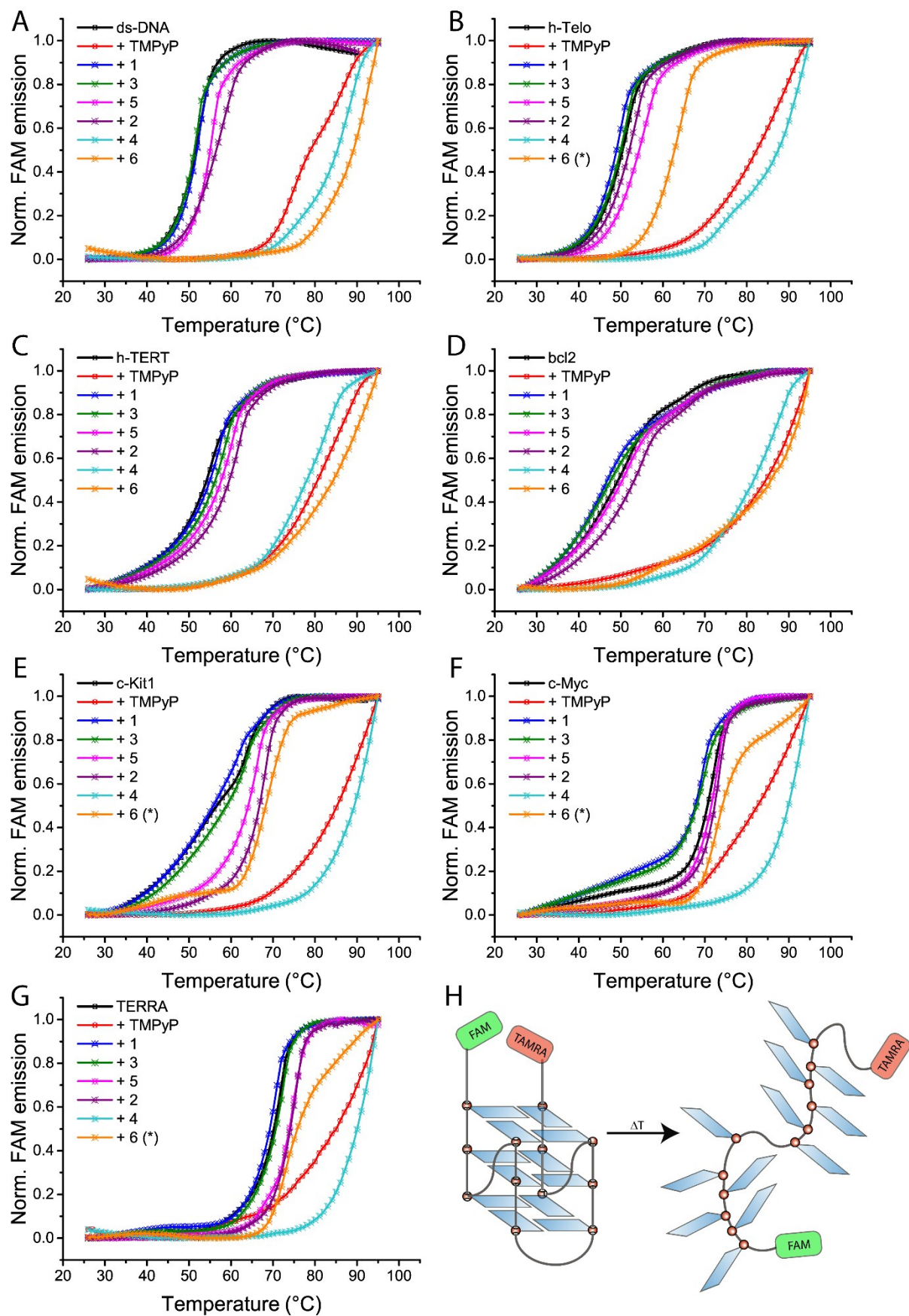


Figure S1. FRET melting profiles of ds-DNA and G4s (0.2 μ M) upon interaction with compounds **1-6** and control TMPyP4 (1.0 μ M; when with * concentration is 0.25 μ M). Buffer: 60 mM potassium cacodylate, pH 7.4.

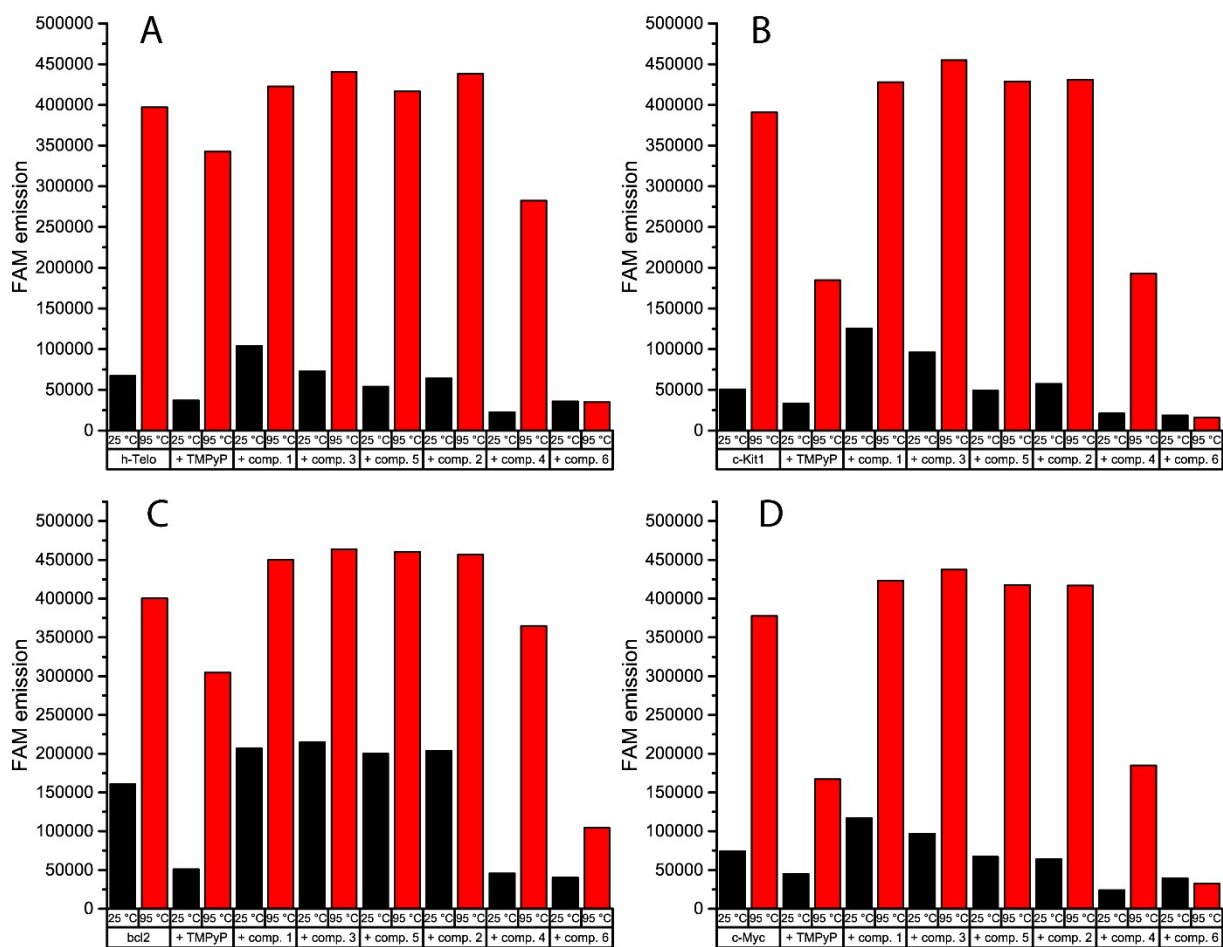


Figure S2. FAM emission at 25.0 and 95.0 °C of selected G4s (0.2 μ M) upon interaction with compound 1-6 and control TMPyP4 (1.0 μ M). Buffer: 60 mM potassium cacodylate, pH 7.4.

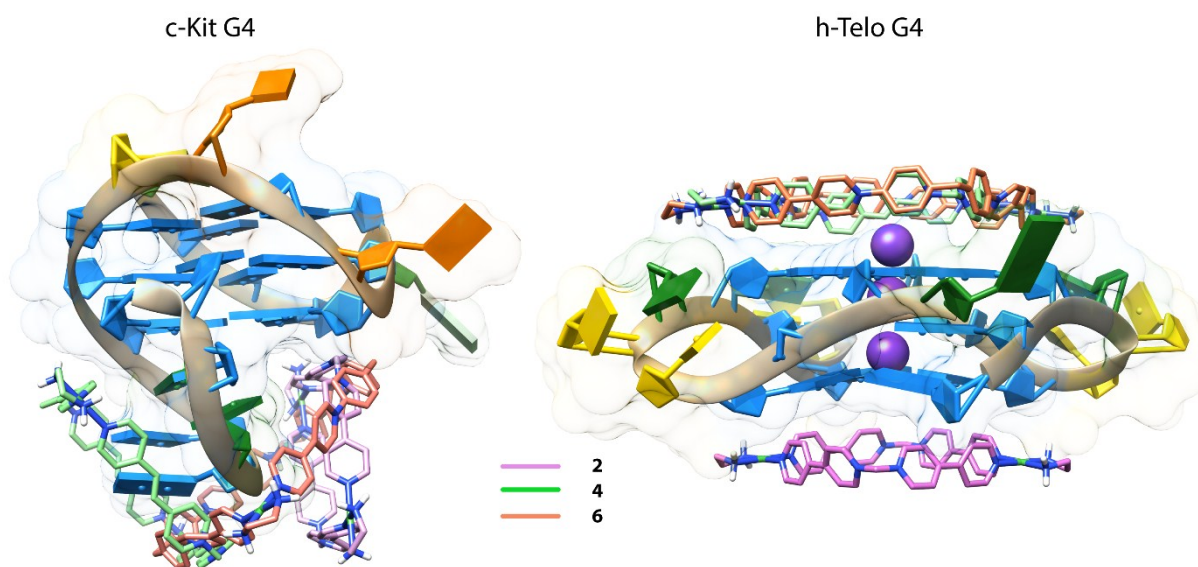


Figure S3. Molecular Docking: cartoon showing possible binding site of 2, 4 and 6 within c-Kit1 (PDB entry 2O3M) and h-Telo (PDB entry 1KF1) G-quadruplexes.

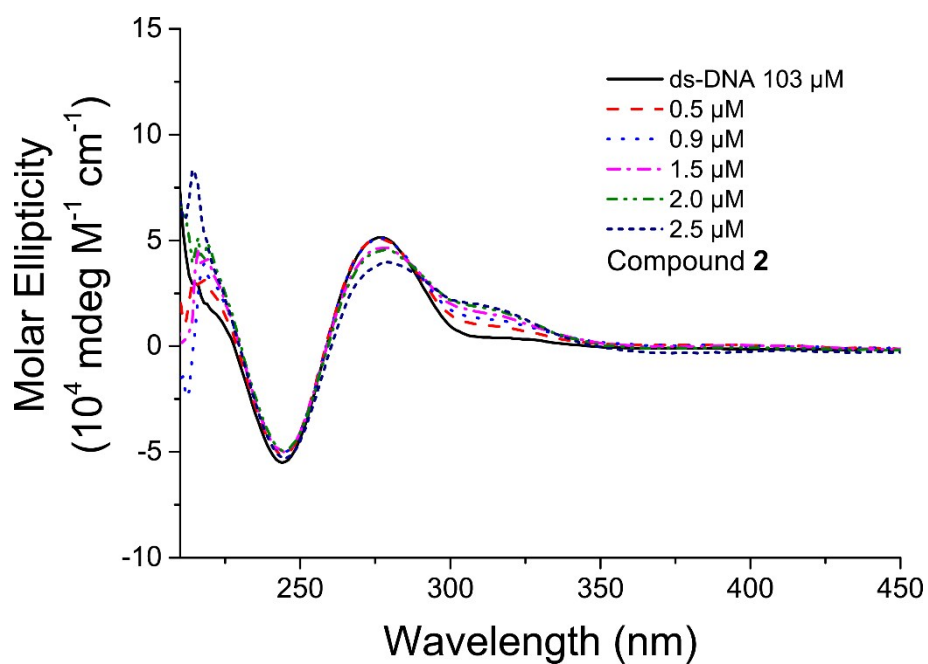


Figure S4. CD titration of ds-DNA with compound **2**. Buffer: 50 mM Tris-HCl and 100 mM KCl, pH 7.4.

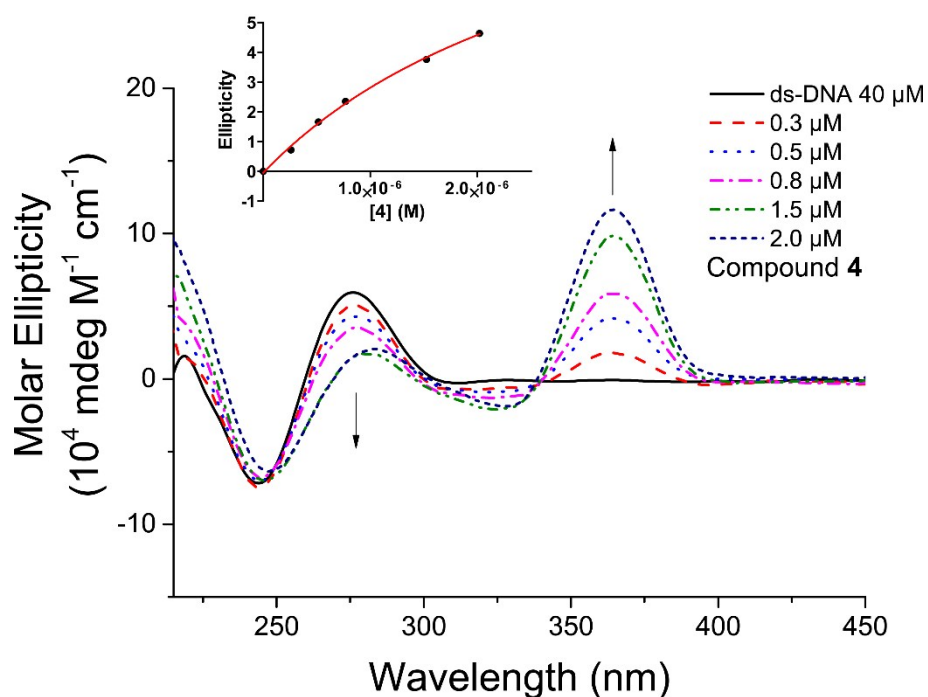


Figure S5. CD titration of ds-DNA with compound **4**. Buffer: 50 mM Tris-HCl and 100 mM KCl, pH 7.4. In the inset the increase in ellipticity at 363 nm vs. **4** concentration. In red the non-linear fit for the estimation of the K_b value ($3.1 \times 10^5 \text{ M}^{-1}$).

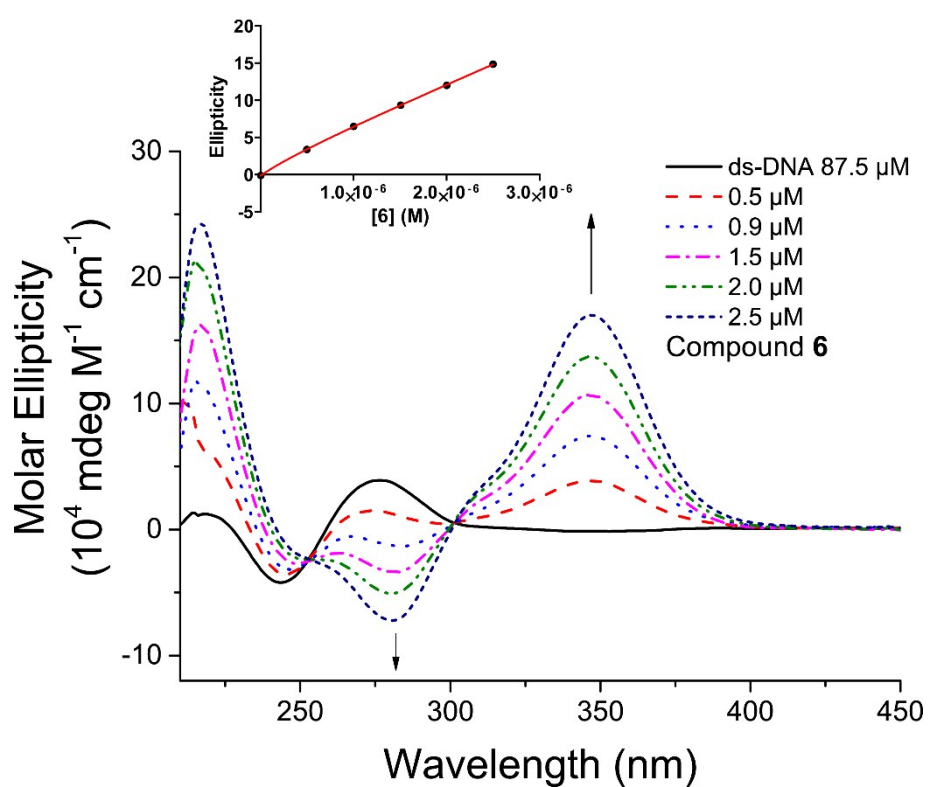


Figure S6. CD titration of ds-DNA with compound **6**. Buffer: 50 mM Tris-HCl and 100 mM KCl, pH 7.4. In the inset the increase in ellipticity at 347 nm vs. **6** concentration. In red the non-linear fit for the estimation of the K_b value ($1.5 \times 10^6 \text{ M}^{-1}$).

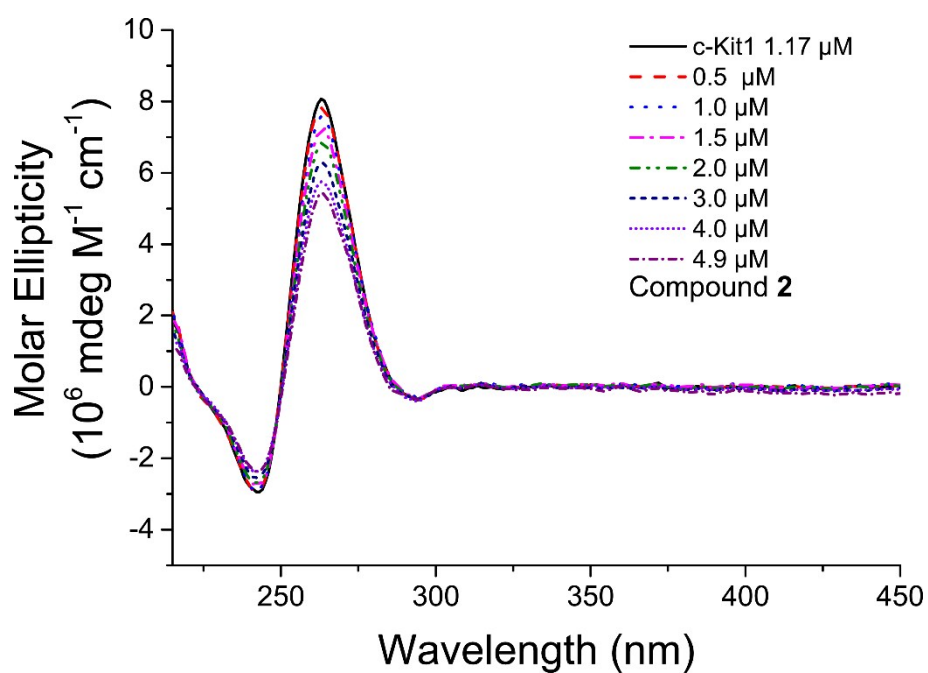


Figure S7. CD titration of c-Kit1 G4 with compound **2**. Buffer: 50 mM Tris-HCl and 100 mM KCl, pH 7.4.

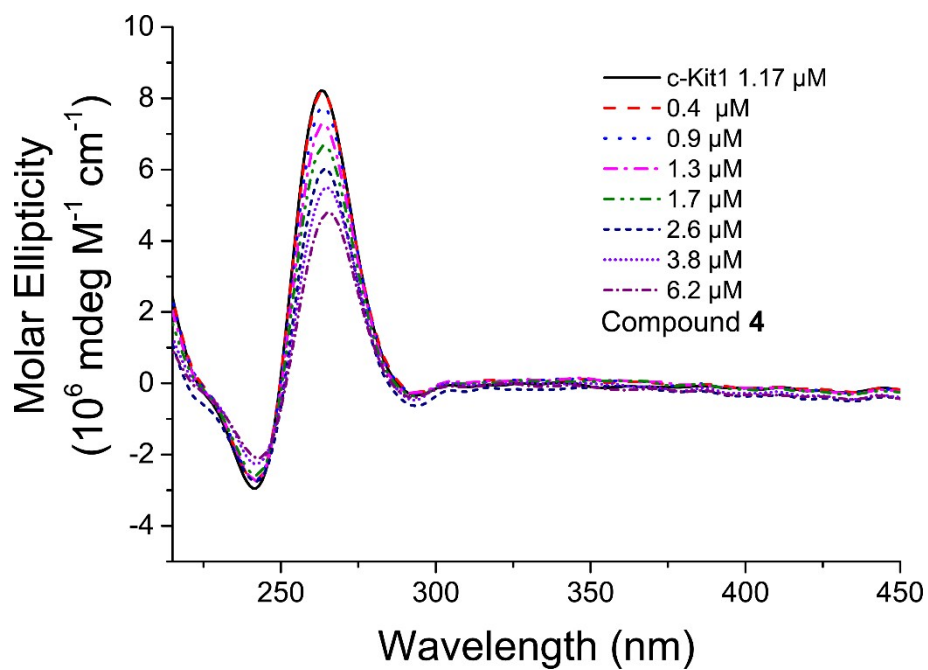


Figure S8. CD titration of c-Kit1 G4 with compound **4**. Buffer: 50 mM Tris-HCl and 100 mM KCl, pH 7.4.

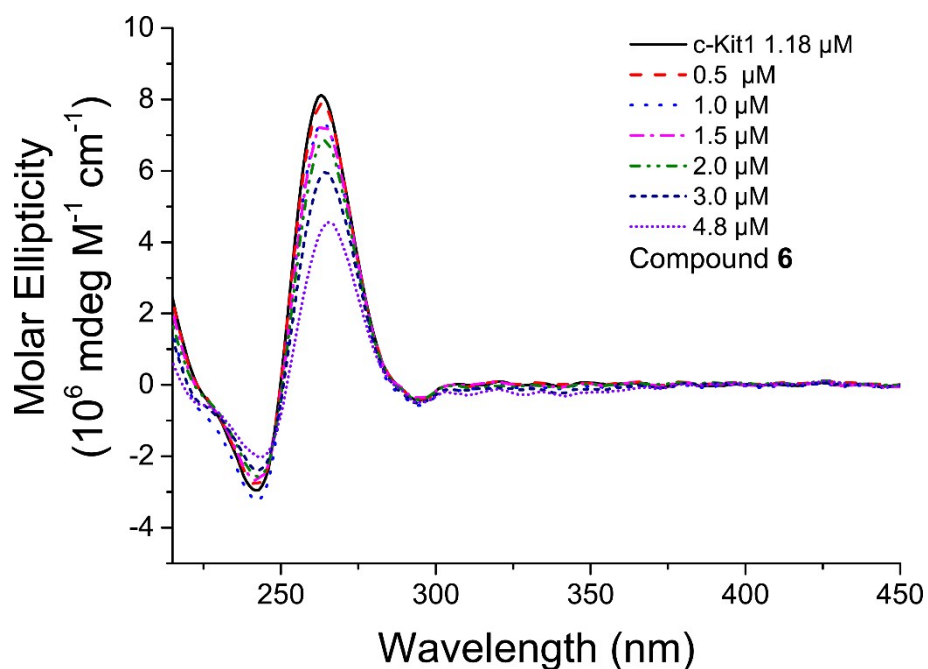


Figure S9. CD titration of c-Kit1 G4 with compound **6**. Buffer: 50 mM Tris-HCl and 100 mM KCl, pH 7.4.

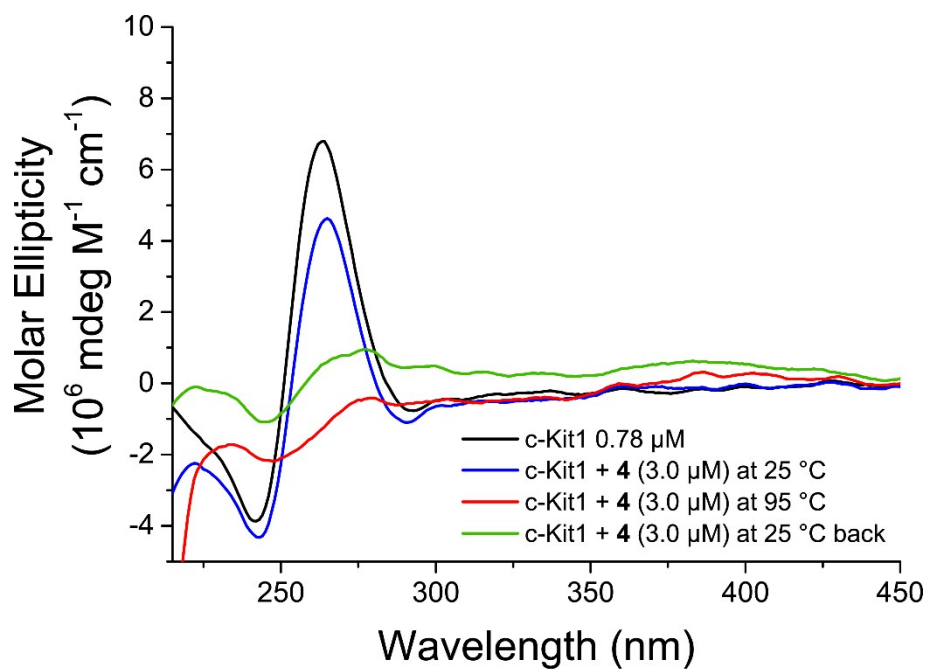


Figure S10. Circular dichroism spectra c-Kit1 G4 in presence of increasing amounts of **4** at 25 $^\circ\text{C}$ and at 95 $^\circ\text{C}$ after unfolding. Buffer: 50 mM Tris-HCl and 100 mM KCl, pH 7.4.

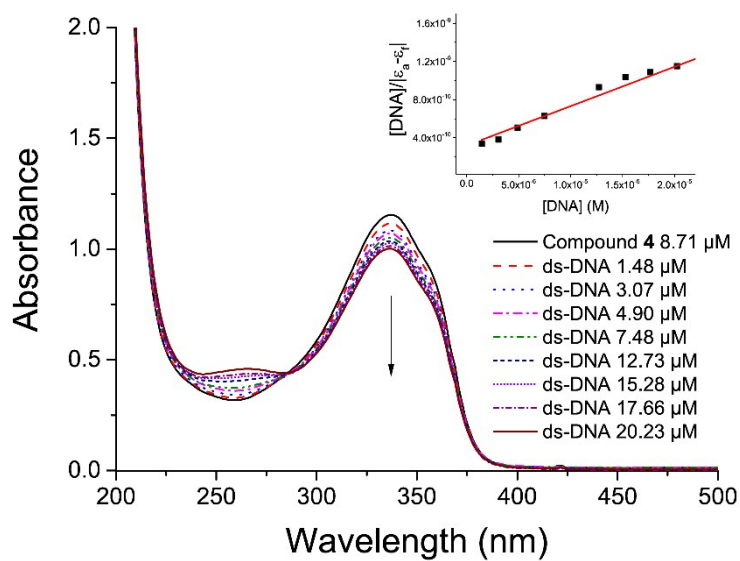


Figure S11. UV-Vis titration of compound **4** with ds-DNA. In the inset the plot of the data with fitting line (in red) for the determination of the K_b value. Buffer: 50 mM Tris-HCl and 100 mM KCl, pH 7.4.

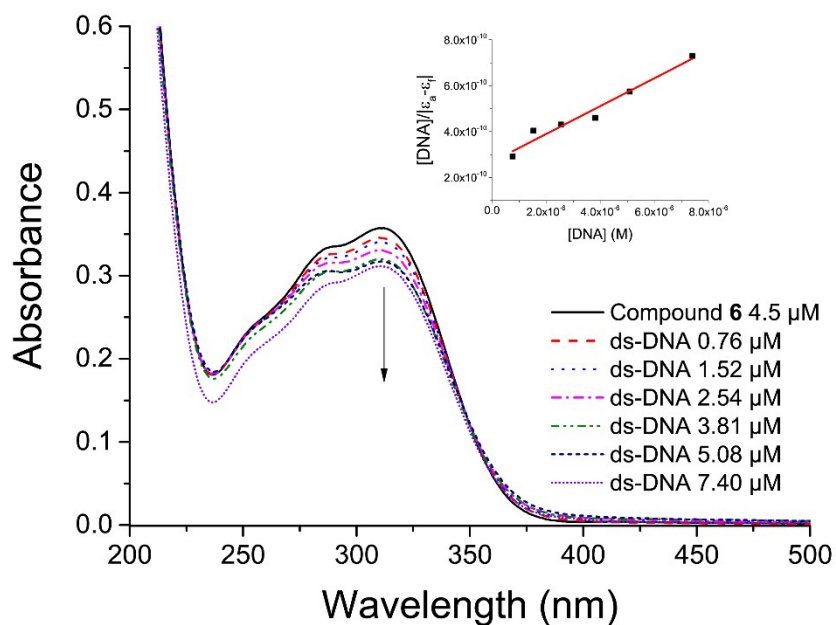


Figure S12. UV-Vis titration of compound **6** with ds-DNA. In the inset the plot of the data with fitting line (in red) for the determination of the K_b value. Buffer: 50 mM Tris-HCl and 100 mM KCl, pH 7.4.

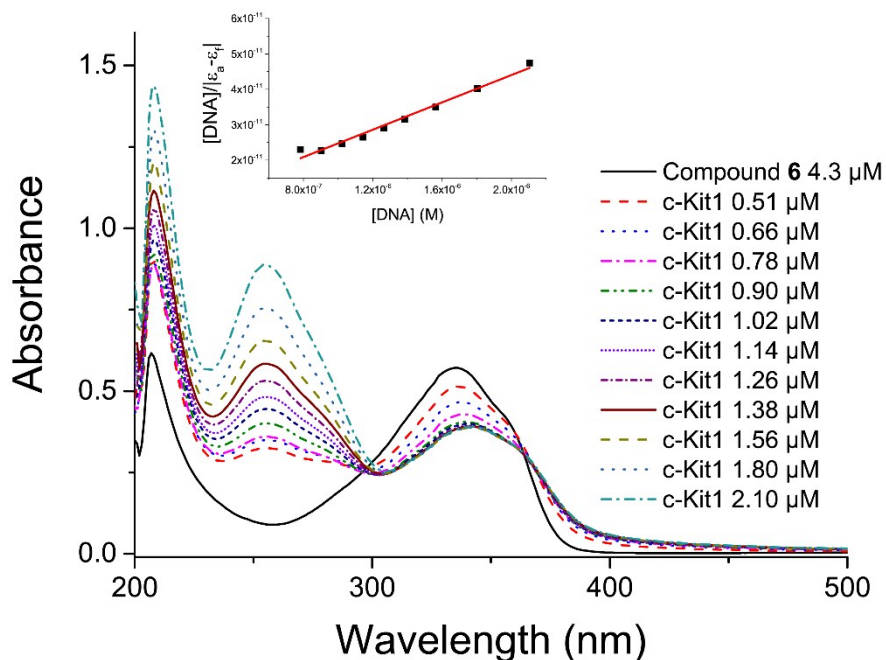


Figure S13. UV-Vis titration of compound **4** with c-Kit1 G4. In the inset the plot of the data with fitting line (in red) for the determination of the K_b value. Buffer: 50 mM Tris-HCl and 100 mM KCl, pH 7.4.

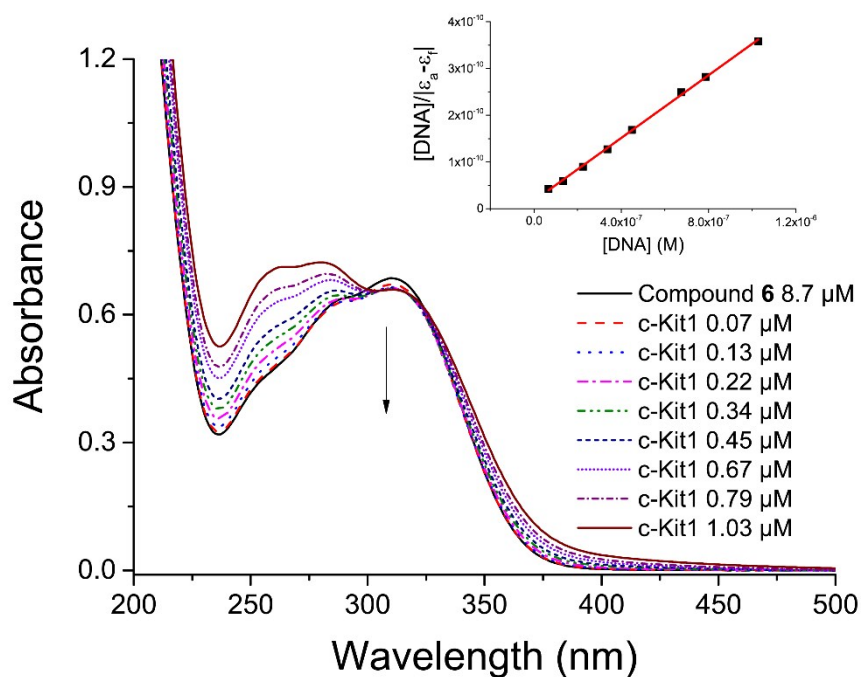


Figure S14. UV-Vis titration of compound **6** with c-Kit1 G4. In the inset the plot of the data with fitting line (in red) for the determination of the K_b value. Buffer: 50 mM Tris-HCl and 100 mM KCl, pH 7.4.

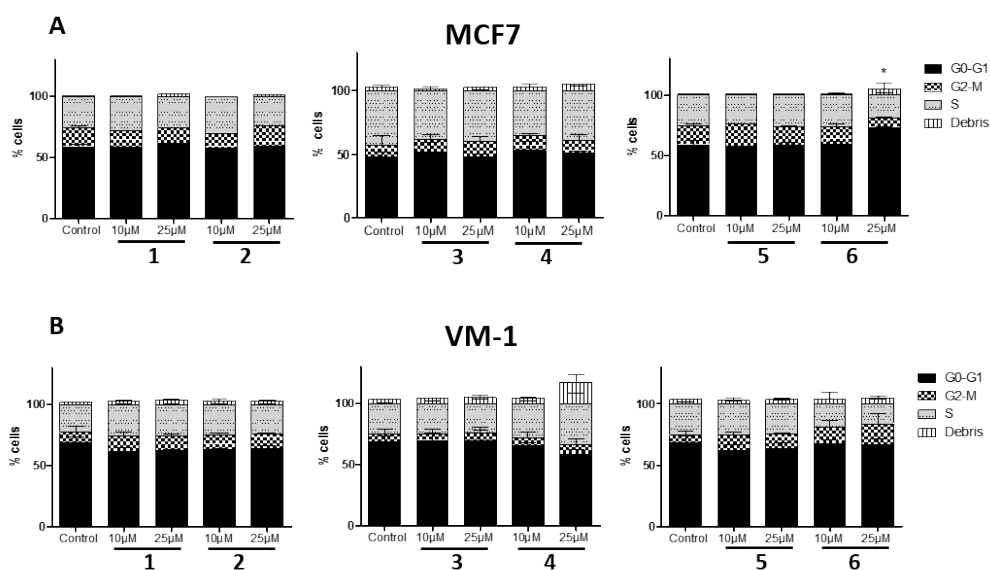


Figure S15. Impact of Pt boxes and their respective ligands on cell cycle distribution in cancer cell lines. MCF-7 breast cancer (A) or VM-1 melanoma cells (B) were treated with the active Pt drugs (**2**, **4** and **6**) as well as with the corresponding ligands (**1**, **3** and **5**) at the indicated concentrations for 48 hours. To evaluate changes in cell cycle distribution FACS analyses were performed and the percentages of cells in G0/G1, S, and G2/M phase were quantified. The means and SD of two independent results are depicted. Statistical analyses were performed between active Pt boxes and their respective ligands using Student's t-test. * $p < 0.05$.

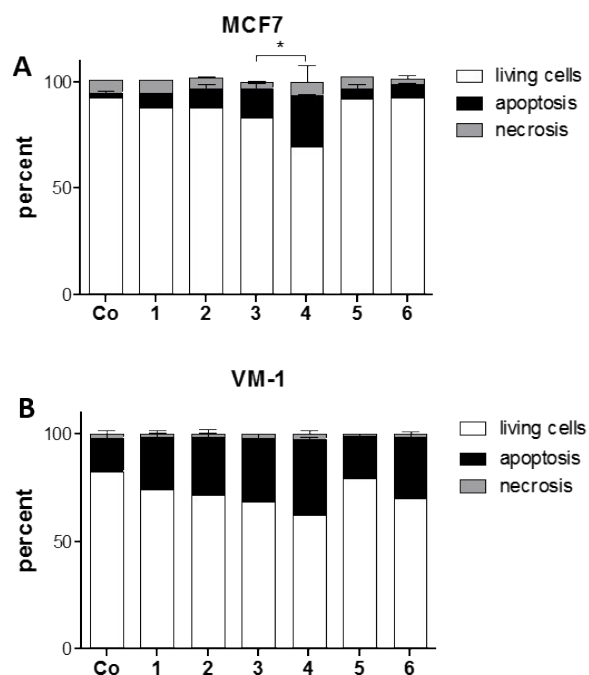


Figure S16. Impact of Pt boxes and their respective ligands on apoptosis and necrosis induction. The percentage of living, apoptotic and necrotic cells were determined by Annexin V/PI staining in MCF7 (A) and VM-1 cells (B) after 24 hours treatment with 25 μM of the indicated drugs. Statistical analyses were performed between active Pt boxes and their respective ligands using Student's t-test. * $p < 0.05$.

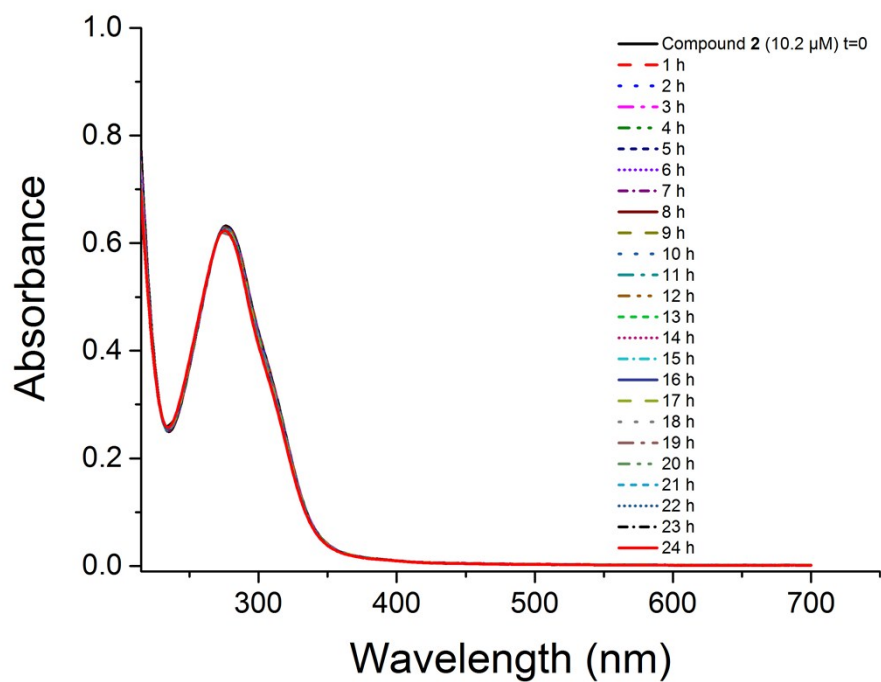


Figure S17. UV-vis spectra of compound 2 overtime to check its stability in buffer solution at 25 $^{\circ}\text{C}$. Buffer: 50 mM Tris-HCl and 100 mM KCl, pH 7.4.

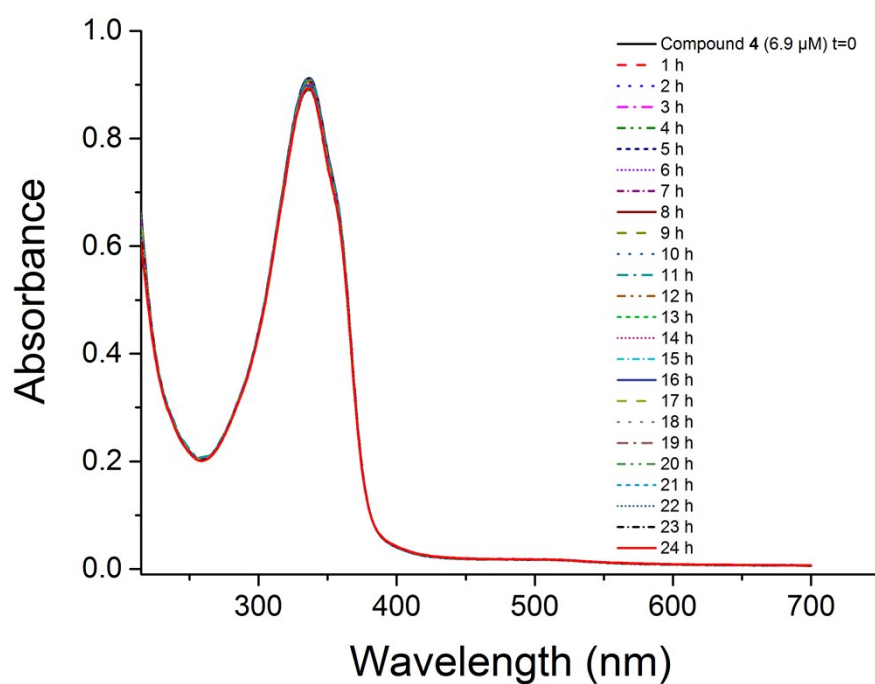


Figure S18. UV-vis spectra of compound **4** overtime to check its stability in buffer solution at 25 °C. Buffer: 50 mM Tris-HCl and 100 mM KCl, pH 7.4.

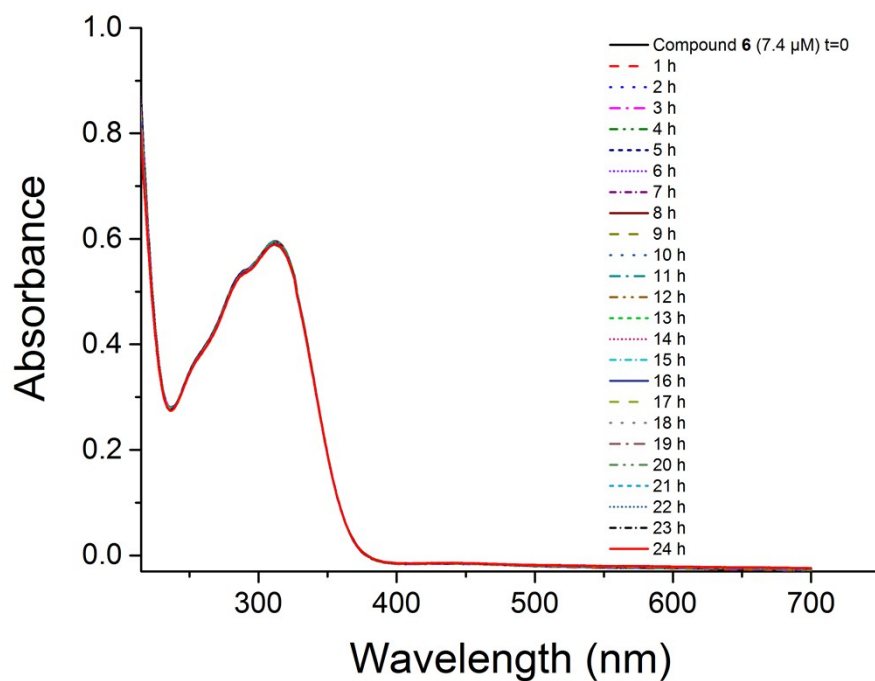


Figure S19. UV-vis spectra of compound **6** overtime to check its stability in buffer solution at 25 °C. Buffer: 50 mM Tris-HCl and 100 mM KCl, pH 7.4.